

Gold–platinum alloy nanoparticle assembly as catalyst for methanol electrooxidation

Yongbing Lou, Mathew M. Maye, Li Han, Jin Luo and Chuan-Jian Zhong*

Department of Chemistry, State University of New York at Binghamton, Binghamton, New York 13902, USA.
E-mail: cjzhong@binghamton.edu

Received (in Columbia, MO, USA) 24th October 2000, Accepted 18th January 2001

First published as an Advance Article on the web 19th February 2001

This paper describes preliminary findings of a thiolate-capped gold–platinum alloy nanoparticle assembly (metallic core and organic shell) as a novel catalyst for electrooxidation of methanol.

The study of catalytic oxidation of methanol and carbon monoxide has broad technological applications, including fuel-cell technology, purification of air in gas products and in long duration space travel, and conversion in automobile exhaust systems.^{1–3} The search for highly effective catalysts and detailed mechanistic understanding^{4–7} has spanned to the exploration of nanometer-size catalysts.^{1–3} Two critical issues facing the exploration of nanosized catalysts for methanol oxidation are however the propensity of poisoning at traditional platinum group catalysts by adsorbed CO-like species and the tendency of nanoparticle aggregation. To address these issues, we have recently reported a proof-of-concept demonstration of electrocatalytic oxidation of CO at core–shell nanostructured alkyl thiolate-capped gold nanoparticles,⁸ a new expansion of recent interest in exploring nanosized bare gold catalysts.^{4,5} We report herein preliminary findings of an investigation of thiolate-encapsulated gold–platinum (Au–Pt) alloy nanoparticles as catalysts for methanol electrooxidation (Scheme 1). In addition to aggregation-resistant and poison-resistant properties arising from shell encapsulation and networking, an important attribute is the bimetallic core composition with different catalytic functions: methanol oxidation at Pt-sites and CO oxidation at Au-sites. Whether such encapsulated alloyed nanosites are catalytically active under the encapsulation is a critical question. The basic understanding will also be useful to much of the recent interest in Pt–Ru based bimetallic catalysts¹ and other related systems such as polypyrrole-supported^{9,10} and dendrimer-encapsulated¹¹ Pt nanoparticles.

The catalyst preparation involved Schiffrin's two-phase synthesis of thiolate-capped gold and alloy nanoparticles.^{12,13} Fig. 1 shows a transmission electron microscopic (TEM) image of decanethiolate (DT) encapsulated Au–Pt nanoparticles which were synthesized from a 5 : 1 feed ratio (Au : Pt) of HAuCl_4 and K_2PtCl_6 . The average core size determined was $ca. 2.5 \pm 0.4$ nm. The UV–VIS spectrum of the nanoparticles showed a subtle difference of surface plasmon resonance band intensity from Au nanoparticles ($ca. 2$ nm) synthesized under similar conditions, consistent with the presence of Pt in the Au nanoparticles.¹³ On the basis of previous XPS data that showed a 1 : 0.3 ratio of

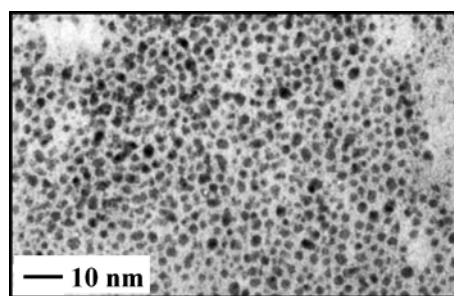
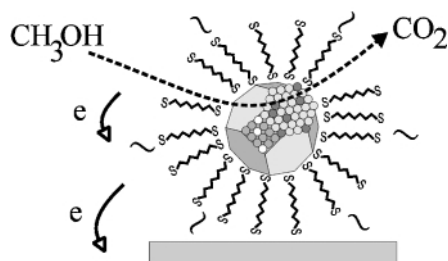


Fig. 1 TEM micrograph of DT-capped Au–Pt (5 : 1) nanoparticles.

Au : Pt in the nanoparticles synthesized from a 1 : 1 feed ratio,¹³ the Pt content estimated for our alloy nanoparticles was $ca. 5\%$. Using 1,9-nonanedithiol (NDT) as the crosslinking agent, the nanoparticles were assembled on a glassy carbon (GC) electrode surface as a shell-linked particle ensemble *via* an exchange–crosslinking–precipitation route.¹⁴ Briefly, a GC electrode was immersed into a hexane solution of DT-capped nanoparticles (30 mM) and NDT (50 mM) for $ca. 24$ h. The NDT–DT exchange reaction was followed by crosslinking, leading to nucleation and growth of a nanoparticle thin film on GC, *i.e.* NDT–(Au–Pt)_{2.5-nm}. The thickness of the film was controlled by immersion time. A typical film had $ca. 8$ equivalent number of particle layers, estimated from quartz-crystal microbalance measurements.¹⁴ Electrochemical measurements were performed in a conventional three-electrode cell with Ag/AgCl (saturated KCl) as reference electrode. The electrolyte solution was purged with argon before measurements.

As recently demonstrated for the case of CO oxidation,⁸ the NDT–(Au–Pt)_{2-nm}/GC electrode was initially activated in the presence of methanol by potential polarization to $ca. 0.8$ V. Fig. 2 shows a typical set of cyclic voltammetric curves [(b)–(e)] at such an activated electrode in an alkaline solution of methanol (99.99%) purged with argon. Curve (a) is the result obtained after transferring the electrode to methanol-free electrolyte. In the absence of methanol (a), the voltammetric curve displays a small and broad oxidation wave at +300 mV extending to the positive potential limit, and a sharp reduction wave at +120 mV. These two waves are attributed to the formation and reduction of surface Au oxide (AuO_x)⁸ on the nanocrystals. Contribution from Pt oxide should be minimal because its redox potential is more positive than that of Au oxide and the alloyed Pt is a very small fraction ($ca. 5\%$). The shell encapsulation may become partially open as a result of either surface oxide formation or a change in shell packing due to possible thiolate desorption or reorganization. In the presence of methanol of different concentrations [(b)–(e)], two voltammetric features are remarkable. First, a large anodic wave is evident at +300 mV. The anodic peak current (i_{pa}) increases with increasing methanol concentration, exhibiting a linear relationship (Fig. 2, insert). The peak potential closely matches the potential for Au oxide formation, suggesting the participation of Au oxide in the overall catalytic oxidation mechanism. An integration of the



Scheme 1 A schematic illustration of catalytic oxidation of methanol at a thiolate-capped core–shell nanoparticle catalyst.

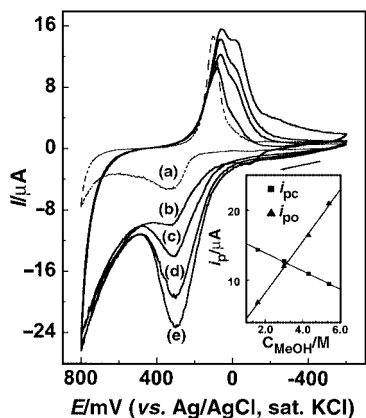


Fig. 2 Cyclic voltammograms for an activated NDT-(Au-Pt)_{2.5-nm}/GC electrode in an electrolyte solution of 0.5 M KOH with methanol concentration of 0 (a), 1.6 M (b), 3.0 M (c), 4.3 M (d) and 5.4 M (e). Geometric electrode area: 0.07 cm². Scan rate: 50 mV s⁻¹.

charge from the cathodic wave translates to *ca.* 9×10^{-9} mol cm⁻² of the amount of reactive Au. Second, in contrast to the trend for the anodic wave, the peak current for the cathodic wave (*i*_{pc}) decreases with increasing methanol concentration, which also exhibits a linear relationship (Fig. 2 insert). These two features are the first set of evidence demonstrating that methanol is oxidized at the nanostructured catalyst. The opposite trend between the oxidation and reduction peak currents as a function of methanol concentration is suggestive of a catalytic mediation mechanism likely by surface Au oxide species.⁶⁻⁸

There is another distinctive feature for the data in comparison with voltammetric characteristics reported for bulk Pt. No oxidation wave is detected in the negative-going sweep of the above data, which is usually observed for Pt-based catalysts due to methanol oxidation at partially reduced surface oxide. Although such an oxidation wave becomes evident at *ca.* -100 mV for a slower scan rate for NDT-(Au-Pt)_{2.5-nm} (Fig. 3), the relative magnitude of the wave is much smaller. We also note that the overall potential of methanol oxidation is *ca.* 200 mV more positive for the NDT-(Au-Pt)_{2.5-nm} than Pt. This difference is presumably due to a conductivity effect of the film.¹⁴

Fig. 3 shows the voltammetric dependence on scan rate (*v*) as a further piece of evidence for the electrocatalytic mediation of the catalyst. Both *i*_{pa} and *i*_{pc} increase with increasing *v*. A close examination reveals that the *i*_{pa} vs. *v*^{1/2} relationship is approximately linear for *v* > 20 mV s⁻¹, indicative of a diffusion-controlled process for methanol oxidation. Remarkably, the ratio of *i*_{pa}:*i*_{pc} decreases with increasing *v*, which is characteristic of an surface redox-mediated catalytic oxidation process. At *v* < 20 mV s⁻¹, the reduction wave basically disappears whereas a small anodic wave is evident on the negative-going sweep. This feature resembles those observed for electrooxidation of methanol at a Pt-based surface³ and of CO at core-shell Au nanoparticle assemblies.⁸ Overall, the data further support an electrocatalytic mechanism by which the oxidation of methanol is mediated by surface oxide redox species.⁶

Other preliminary data are also supportive of the above assessment. An insignificant change of C-H stretching bands of alkyl thiolates in IR reflection spectroscopic data before and after the catalytic activation supports the presence of shell encapsulation. Voltammetric data with a similar catalytic activity but different characteristics have also been noticed using thiolate-capped Au nanoparticles, which is under further

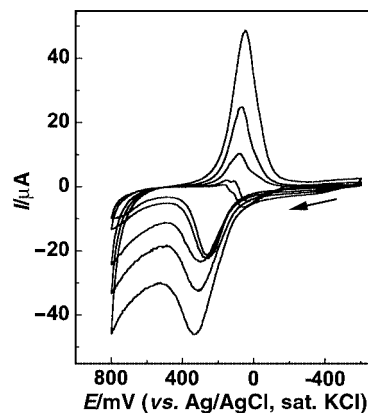


Fig. 3 Scan rate dependence of cyclic voltammograms for an activated NDT-(Au-Pt)_{2.5-nm}/GC electrode in a solution of 0.5 M KOH + 5.4 M methanol. Geometric electrode area: 0.07 cm². Scan rate: 10, 20, 50, 100 and 200 mV s⁻¹. Both anodic peak and cathodic currents increase with increasing scan rate.

investigation. Moreover, the catalytic activity is remarkably stable against repetitive cycling (at least 2 h at 10–200 mV s⁻¹) in the indicated potential region. We believe that the catalytic oxidation proceeds predominantly at surface Au oxide sites within the core-shell nanoparticle assembly. As reviewed recently by Burke and Nugent⁶ for gold-based catalysis, oxygen transfer reactions have been considered using an incipient hydrous oxide/adatom mediator model. In a few recent examples, metal oxides are used as supports for bare Au nanoparticle catalysts.⁵

The result is, to our knowledge, the first example of electrocatalytic oxidation of methanol at core-shell nanostructured Au-Pt nanoparticles upon catalytic activation. A systematic manipulation of the bimetallic core composition is under way, including further investigations using nanoparticle size and shape processing methods,¹⁵ IR reflection spectroscopy and atomic force microscopy to gain insights into effects of nanostructured voids, nanocrystal corners or edges, surface activation and segregation.

The ACS Petroleum Research Fund is acknowledged for support of this research.

Notes and references

- S. Wasmus and A. Kuever, *J. Electroanal. Chem.*, 1999, **461**, 14.
- Electrocatalysis, Frontiers in Electrochemistry*, ed. J. Lipkowsky and P. N. Jr. Ross, VCH, New York, 1997, vol. 5.
- T. D. Jarvi, S. Sriramulu and E. M. Stuve, *J. Phys. Chem. B.*, 1998, **101**, 3649.
- M. Valden, X. Lai and D. W. Goodman, *Science*, 1998, **281**, 1647.
- M. Haruta, *Catal. Today*, 1997, **36**, 153.
- L. D. Burke and P. F. Nugent, *Gold Bull.*, 1998, **31**, 39.
- G. C. Bond, *Catal. Rev.*, 1999, **41**, 319.
- M. M. Maye, Y. Lou and C. J. Zhong, *Langmuir*, 2000, **16**, 7520.
- M. Hepel, *J. Electrochem. Soc.*, 1998, **145**, 124.
- P. J. Kulesza, M. Matczak, A. Wolkiewicz, B. Crzybowska, M. Galkowski, M. A. Malik and A. Wieckowski, *Electrochim. Acta*, 1999, **44**, 2131.
- M. Q. Zhao and R. M. Crooks, *Adv. Mater.*, 1999, **11**, 217.
- M. Brust, M. Walker, D. Bethell, D. J. Schiffrin and R. Whyman, *J. Chem. Soc., Chem. Commun.*, 1994, 801.
- M. J. Hostetler, C. J. Zhong, B. K. H. Yen, J. Anderegg, S. M. Gross, N. D. Evans, M. D. Porter and R. W. Murray, *J. Am. Chem. Soc.*, 1998, **120**, 9396.
- F. L. Leibowitz, W. X. Zheng, M. M. Maye and C. J. Zhong, *Anal. Chem.*, 1999, **71**, 5076.
- M. M. Maye, W. X. Zheng, F. L. Leibowitz, N. K. Ly and C. J. Zhong, *Langmuir*, 2000, **16**, 490.